

ZnO particles as scattering centers to optimize color production and lumen efficiencies of warm white LEDs

H. T. TUNG¹, B. T. MINH², N. L. THAI³, H. Y. LEE⁴, N. D. Q. ANH^{5,*}

¹Faculty of Basic Sciences, Vinh Long University of Technology Education, Vinh Long Province, Vietnam

²Faculty of Electrical and Electronics Engineering, Nha Trang University, Nha Trang City, Vietnam

³Faculty of Engineering and Technology, Nguyen Tat Thanh University, Ho Chi Minh City, Vietnam

⁴Department of Electrical Engineering, National Kaohsiung University of Sciences and Technology, Kaohsiung, Taiwan

⁵Faculty of Electrical and Electronics Engineering, Ton Duc Thang University, Ho Chi Minh City, Vietnam

This research integrates ZnO particles as essential scattering components within a remote phosphor structure, specifically designed to enhance the performance of warm white LEDs tailored for lighting applications. In this endeavor, an additional layer of red phosphor is intricately incorporated alongside the yellow-phosphor film, wherein the ZnO concentration ranges from 0 wt% to 50 wt%. The study evaluates a spectrum of parameters including scattering properties, lumen output, spatial color distribution consistency (or color uniformity), and chromatic reproduction efficiency. The assessments are simulation-based works carried out with LightTools and MATLAB programs, employing Mie theory in scattering. The findings distinctly underscore the pivotal role of determining optimal ZnO concentrations, which not only contribute to achieving commendable brightness in white light and robust color rendering capabilities but also significantly enhance color uniformity within the illuminated spectrum. This exploration provides invaluable insights into the delicate balance and critical role of ZnO concentration in shaping the overall performance of warm white LED structures for practical lighting applications.

(Received December 10, 2023; accepted June 5, 2024)

Keywords: Color distribution, Color reproduction, Luminous efficacy, Scattering performance, White LED

1. Introduction

The ascension of white light-emitting diodes (LEDs) stands as a monumental milestone in the domain of illumination and display technologies, ushering in an era of energy-efficient, enduring lighting solutions applicable across a wide spectrum of industries [1-3]. The versatile functionality and efficiency of white LEDs have positioned them as the preferred lighting solution across residential, commercial, automotive, and specialized sectors, marking a profound shift from traditional incandescent and fluorescent light sources. Despite the significant advantages of contemporary LED technology, notably the phosphor-converted yellow YAG:Ce³⁺ employed atop blue LED chips, these devices encounter inherent isotropic challenges hampering their performance in both color quality and lumen output [4-6]. Moreover, the vexing issue of light loss due to backscattering limits the efficiency of light extraction, signifying a ratio of escaped photons into the surrounding air versus those generated within the active layer [7, 8]. To overcome these obstacles, the scientific community has extensively explored an array of strategies detailed in academic literature, focusing on the manipulation of photon angles through structured surface scattering or the integration of additional layers with suitable refractive indexes strategically positioned in LED structures [9-11].

Among the multitude of proposed solutions, ZnO has emerged as a focal point of interest due to its promising attributes for LED lighting applications. Exhibiting a wide

and direct bandgap, ZnO serves as an n-type semiconductor with a wide array of technological applications in solid-state lighting, solar cells, and sensor devices. Its customizable nanostructures and refractive index, which conveniently aligns with the RIs of LEDs and air, position ZnO as an appealing option for LED technology [12, 13]. The material's capacity to enhance light scattering further bolsters its potential in LED technology. Additionally, atomic layer deposition of ZnO thin films has been investigated for applications in thin film transistors in transparent and flexible electronics, with controllable growth rates, electrical conductivity, crystal orientation, and visible luminescence.

This research paper aims to vary the amount of doping ZnO into the phosphor films to produce better color-uniformity white LED. A common issue in white LED light production is the deficiency of red color elements, resulting in a colder light that can discomfort human eyes, particularly during daytime use. The integration of Eu³⁺-doped red phosphor materials, such as Eu³⁺-doped Y₂O₂S, has been extensively studied and found feasible to adjust doping levels for desired outcomes [14-16]. By utilizing blue-excited LED chips, red and yellow phosphors, and ZnO thin films as primary components, the investigation delves into the scattering factors, luminous performance, and chromatic rendering properties of LED white lighting. The outcomes emphasize the improvements in specific properties resulting from varying ZnO concentrations, offering valuable insights to propel advancements in LED lighting development.

2. Simulation methods

The configuration of the LED with remote phosphor converter layers is displayed in this investigation. The remote phosphor structure can hinder the significant amount of photons absorbed by the LED chip by utilizing a sufficient distance between the converter film and the chips' surfaces [17]. Thus, in this work, utilizing the remote phosphor configuration serves as a means to improve the light extraction of the LED when varying the ZnO to monitor the light scattering factor. As depicted in Fig. 1, the LED assembly encompasses a unique combination of elements, notably the compound of yellow-phosphor YAG:Ce and ZnO particle situated above the LED chip. Particularly, the 3D simulation of the LED model is depicted in Fig. 1a using LightTools software, and the remote phosphor configuration illustration is in Fig. 1b. This remote phosphor packaging design aims to optimize light conversion, ensuring a more uniform output of white light.

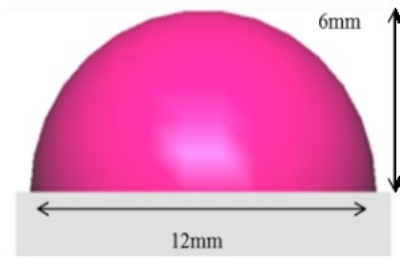
Mie theoretical calculations are applied to analyze ZnO and phosphor particles as spherical entities, thereby deriving their optical constants in accordance with Mie theory [18]. In the simulation, the input of ZnO and YAG:Ce³⁺ concentrations are variables. The other parameters are constant as follows. The excitation source from blue chips is 460 nm. The radii of ZnO and the phosphor materials are 5 μm and 7.25 μm , respectively. The phosphor layer thickness is 0.08 mm. The bandgaps and emission peaks of YAG:Ce³⁺ phosphor, red phosphor, and ZnO are in Table 1.

Table 1. Phosphors and ZnO input parameters

Materials	Particle size	Bandgap	Emission peaks
YAG:Ce ³⁺	7.25 μm [19]	~ 3.7 eV [20]	550-570 nm [21]
Red phosphor (Y ₂ O ₃ :Eu ³⁺)	7.25 μm [19]	5.8 eV [22]	613 nm [22]
ZnO	5 μm [19]	~ 3.37 eV [23]	540 nm [24]

The ZnO content input was changed from 0 wt% to 50 wt% and the concentration of YAG:Ce³⁺ was altered accordingly from 14 wt% to 2 wt%, as illustrated in Fig. 2. The change in these phosphor concentrations is to ensure the fixed thickness of the phosphor layer. Notably, a discernible inverse relationship emerges between the concentration of YAG:Ce phosphor and the presence of ZnO within the compound. Yet, the YAG:Ce³⁺ is likely to lightly increase at first, with ZnO concentration increasing from 0-5 wt%. Beyond 5 wt% ZnO concentration, YAG:Ce³⁺ concentration shows a sustainable decline. This not only facilitates the regulation of scattering activities but also plays a crucial role in stabilizing the LED package's internal temperature during prolonged operational periods. The findings of this study contribute

to the optimization of LED design for enhanced light emission and operational efficiency.



(a)



(b)

Fig. 1. The modelled LED: (a) 3D simulation of the LED by LightTools software and (b) the remote phosphor (color online)

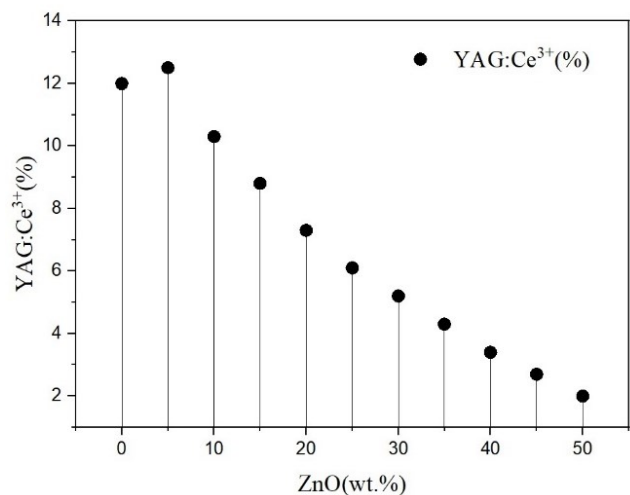


Fig. 2. YAG:Ce³⁺ concentration with varying ZnO contents in the layer

3. Computation and discussion

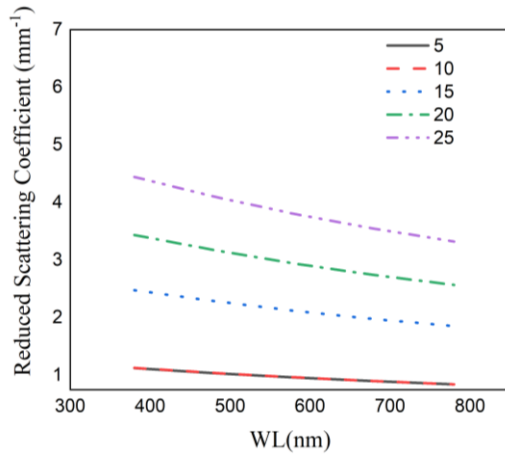
We utilize a Mie-scattering-based computational framework to scrutinize the light scattering phenomena within the phosphor film [25-27], specifically with varying concentrations of ZnO. The central aim was to ascertain the reduced scattering coefficient (δ_{sca}) of the phosphor layer, mathematically expressed through equations 1 and 2. The computation incorporates key parameters including the total distribution density of luminescent particles ($N(r)$), the wavelength of incident light (λ), particle radius

(r), scattering coefficients ($\mu_{sca}(\lambda)$), the anisotropy factor g , and scattering cross-sections (C_{sca}). This rigorous analysis enabled a comprehensive understanding of the intricacies of light scattering within the phosphor layer, shedding light on how different ZnO concentrations affect the scattering behavior and, consequently, the optical performance of the LED structure [28].

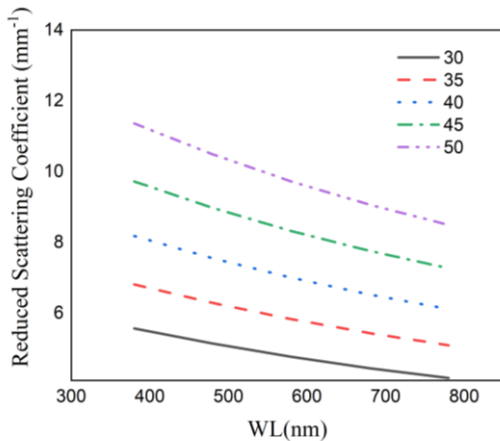
$$\delta_{sca} = \mu_{sca}(1-g) \quad (1)$$

$$\mu_{sca}(\lambda) = \int N(r)C_{sca}(\lambda, r)dr \quad (2)$$

The obtained reduced scattering data are illustrated in Fig. 3. Initially, the small increase of ZnO concentration of 5-10 wt% does not impact much on the scattering factor as two scattering lines in the graph coincide. Further increasing the ZnO amount leads to higher values of the reduced scattering parameter. Besides, the longer wavelength presents a lower scattering strength, which can be demonstrated with Mie-scattering for spherical particles. These results offer a significant insight into the interplay between ZnO concentration and light scattering, presenting a viable strategy for improving the overall optical performance, including luminosity and color fidelity and uniformity of white LED lighting systems.



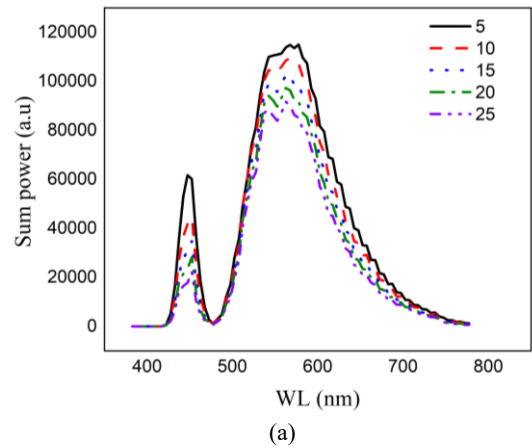
(a)



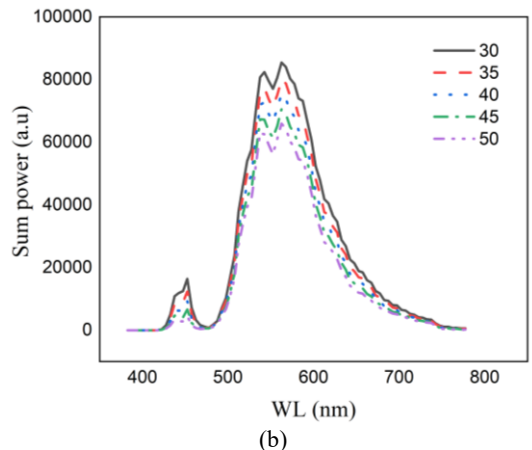
(b)

Fig. 3. Reduced scattering properties with altering concentration of ZnO: (a) 5 nm-25 nm, (b) 30 nm-50 nm (color online)

Fig. 4 shows the light spectral distribution of the LED package with different ZnO contents. The graph represents the wavelength of the emitted light, including blue (425-460 nm) and green to bright red (525-600 nm). Within these bands, multiple emission peaks are observed. The intensity and shape of these peaks change with the concentrations of ZnO in the film. The increase in ZnO concentration induces a drop in the transmission power of the light rays in the LED, which is similar to the data demonstrated in [29]. However, the positions of these peaks remain consistent regardless of changes in the ZnO concentration. As the concentration of ZnO increases, the peaks centered at ~ 435 nm, 455 nm, 545 nm, and 570 nm are more defined while the other seems to be omitted in the collected emission bands. These emission peaks probably come from the ZnO particles (435 nm, 545 nm), blue chips (455 nm), and yellow phosphor (570 nm). The simulated data of ZnO emission peaks in this work relatively match the results of previous papers on other blue-light excitable ZnO-doped compounds [30-33]. It can be observed that the ZnO particles acted as scattering centers, which increased the path length and the probability of interaction between the blue incident light and the phosphors. Moreover, the ZnO particles absorbed the blue light and re-emitted it in as green-colored light (~ 545 nm). Therefore, the ZnO particles play a critical role in stimulating the color mixing and the color uniformity of the white light output.



(a)



(b)

Fig. 4. Transmittance power of the white LED with altering concentration of ZnO: (a) 5 nm-25 nm, (b) 30 nm-50 nm (color online)

The incorporation of ZnO within the design has led to a marginal increase in the correlated color temperature (CCT) range across various viewing angles. Notably, the resulting white light remains within the warm color temperature range at 3900–4025 K, as depicted in Fig. 5. However, it is crucial to highlight the substantial variance observed in the angular CCT ranges across different ZnO concentrations. As the ZnO concentration exceeds 20 wt%, the CCT range stays around 4000 K, accompanied by a notable decline in intensity at the direct viewing angle (0°). This decline suggests an improved dispersion of light towards the edges of the package due to the heightened reduction in scattering efficiency. The most stable-like angular CCT range is associated with a ZnO concentration of 45 wt%, demonstrating the smallest CCT values between the largest ($\pm 60^\circ$) and the direct (0°) viewing angles.

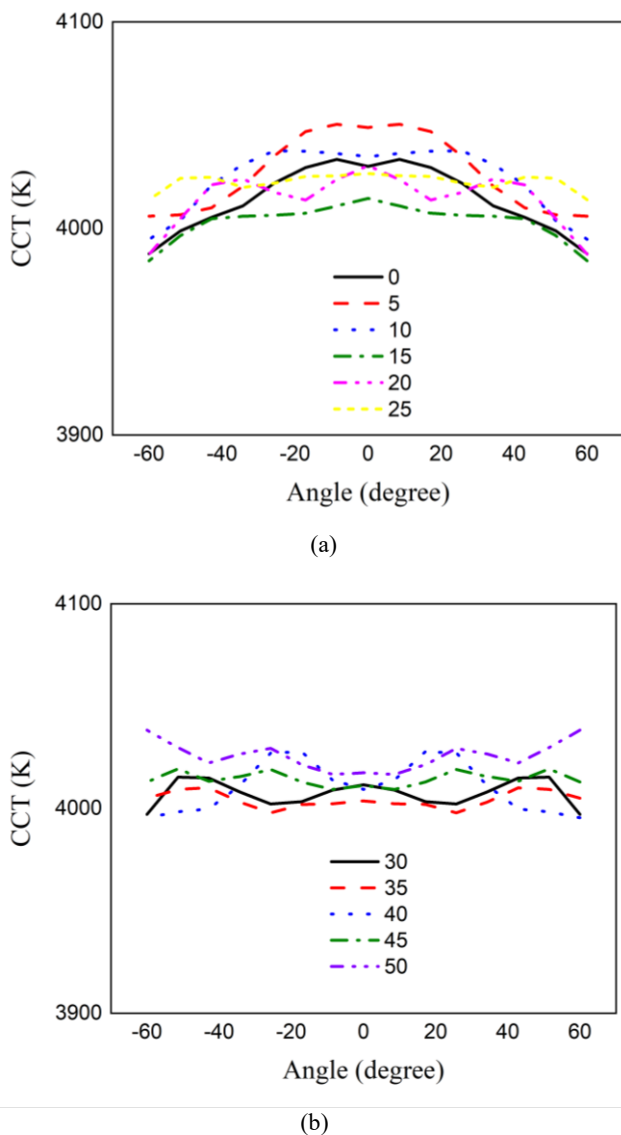


Fig. 5. The CCT range with altering concentration of ZnO: (a) 5 nm–25 nm, (b) 30 nm–50 nm (color online)

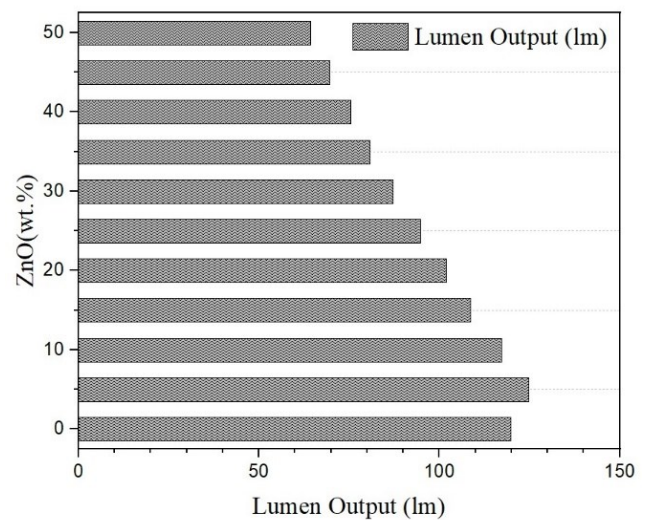


Fig. 6. Lumen changes with altering concentration of ZnO

Nevertheless, an increase in ZnO concentration results in a noticeable decline in the intensity of the entire emission band, referring Fig. 4. This decrease in transmittance power can be attributed to energy loss caused by both scattering and absorption within the phosphor sheets. The reduction in transmittance power could adversely impact the lumen output of the white LEDs. Fig. 6 illustrates the lumens produced by the white LEDs at varying ZnO concentrations. It becomes evident that the addition of 5 wt% ZnO enhances the lumen output, since at this concentration, the transmittance peaks are the most intense (see Fig. 4). This result indicates that 5 wt% of ZnO favors a stronger utilization and extraction of blue light due to effective forward scattering capabilities. However, elevating the ZnO concentration beyond this point leads to reduced transparency within the phosphor film, diminishing light transmittance efficiency. Moreover, the heightened ZnO concentrations induce increased scattering, resulting in multiple scattering events that progressively reduce the light's energy, ultimately decreasing the overall lumen output of the LED. Consequently, beyond 5 wt% of ZnO concentration, the lumen output of the white LED declines, indicating the delicate balance between ZnO concentration and optimal luminosity in LED design.

The uniformity of color holds substantial importance in the development of high-quality white LED devices, given that white light with superior color consistency tends to be more visually pleasing and comfortable for human eyes. The delta-CCT, which quantifies the variance between the highest and lowest CCT levels, as displayed in Fig. 7, serves as a measure of color variation. Generally, the incorporation of ZnO films supports enhanced color dispersion due to improved scattering properties. The lowest delta-CCT, indicating the highest uniformity, is achieved at 45 wt% ZnO, exhibiting a reduction of ~ 75 K compared to the reference data. Furthermore, the delta-CCT with the use of 20–25 wt% and 50 wt% ZnO is lower than reference value. Conversely, the highest delta-CCT, signifying the least uniformity in chromatic distribution, is

associated with a ZnO concentration of 15 wt%. Shortly, for optimal color uniformity, the ideal ZnO concentration should be 45 wt% or at least fall within the range of 20-25 wt%.

Additionally, the improvement in blue light scattering and absorption with increasing ZnO concentration can support the color-reproduction enhancement by intensifying the amount of converted red light. Figs. 8 and 9 present a comprehensive overview of the Color Quality Scale (CQS) and Color Rendering Index (CRI) performance concerning varying concentrations of ZnO. Notably, at 5 wt% ZnO, a significant enhancement is observed compared to cases without ZnO films, demonstrating ZnO's capacity to improve the chroma reproduction performance of white LED light. This concentration, at 5 wt%, showcases sufficient scattering and conversion efficiencies, resulting in broader color coverage on the chroma spectrum. Consequently, the generated light is capable of rendering more color elements of the targeted object. However, a consistent trend emerges as ZnO concentration increases beyond 5 wt%, revealing a gradual reduction in both CRI and CQS parameters, even lower than the reference data [34, 35].

This observed trend of color-reproduction parameters is in alignment with the behavior noted in the lumen strength of the white LED. Higher concentrations of ZnO seem to promote the absorption of blue light and the emission of red light, leading to a noticeable shift in the overall emission color spectrum toward the yellow-red range. This shift likely contributes to a decline in color reproduction quality due to the reduced presence of blue light [36, 37]. Hence, these findings underline that the most favorable ZnO concentration for both lumen output and color rendition is at 5 wt%. This concentration not only enhances color reproduction but also maintains a balance between color quality and the overall luminosity of the white LED.

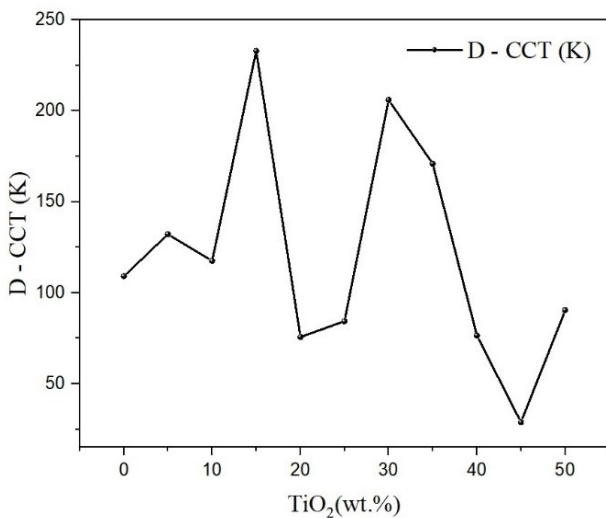


Fig. 7. The CCT delta with altering concentration of ZnO

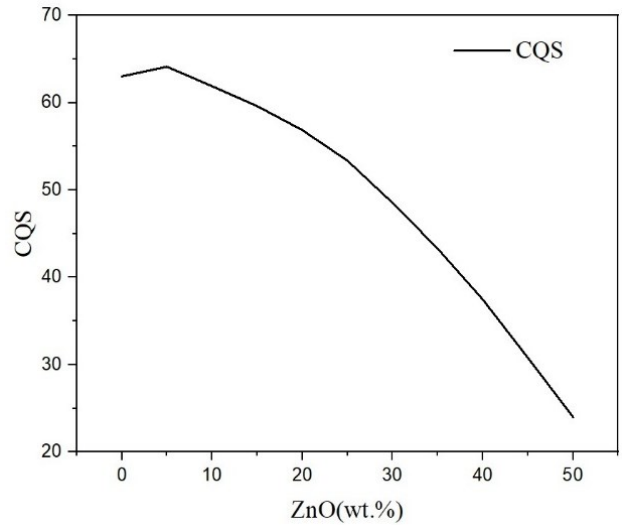


Fig. 8. CQS with altering concentration of ZnO

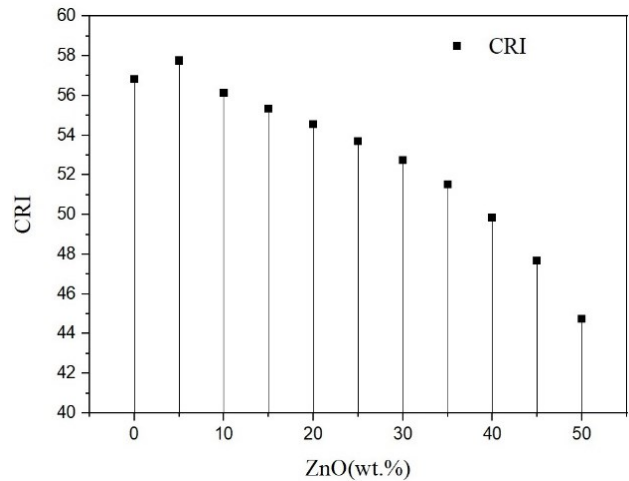


Fig. 9. CRI with altering concentration of ZnO

4. Conclusions

This research paper centers on the integration of ZnO particles as scattering agents within a remote phosphor structure, aimed at improving the overall performance of the warm white LED tailored for lighting applications. As the concentration of ZnO increases, it markedly improves the scattering function, resulting in a more even dispersion of colors and heightened overall color uniformity. Our simulation study indicates that the optimal ZnO concentration for minimizing spatial color deviation is about 45 wt%. Additionally, using ZnO concentration range of 20-25 wt% helps achieve superior color uniformity compared to the reference data within the scope of our research. Concurrently, the investigation identifies 5 wt% ZnO as the suitable quantity for maintaining respectable lumen strength and efficient color rendering. However, beyond 5 wt% ZnO, these parameters experience a decline due to reduced luminous energy following each scattering event and a lack of blue-light emission, ultimately contributing to color deviation. These

findings highlight the delicate balance in ZnO concentration crucial for achieving both enhanced color uniformity and satisfactory lumen output with efficient color rendition in warm white LED designs.

References

- [1] T. Wei, W. Bo, C. Yan, C. Yeqing, L. Jun, Z. Qingguang, *Opt. Mater. Express* **9**, 223 (2019).
- [2] J. Miao, M. Chen, Z. Chen, L. Zhang, S. Wei, X. Yang, *Appl. Opt.* **60**, 1508 (2021).
- [3] B. Wang, D. S. Li, L. F. Shen, E. Y. B. Pun, H. Lin, *Opt. Mater. Express* **9**, 1749 (2019).
- [4] J. X. Yang, D. S. Li, G. Li, E. Y. B. Pun, H. Lin, *Appl. Opt.* **59**, 5752 (2020).
- [5] D. Chen, S. Miao, Y. Liang, W. Wang, S. Yan, J. Bi, K. Sun, *Opt. Mater. Express* **11**, 355 (2021).
- [6] H. E. A. Mohamed, K. Hkiri, M. Khenfouch, S. Dhlamini, M. Henini, M. Maaza, *J. Opt. Soc. Am. A* **37**, C73 (2020).
- [7] X. Huang, X. Zhao, Z. Yu, Y. Liu, A. Wang, X. Wang, F. Liu, *Opt. Mater. Express* **10**, 1163 (2020).
- [8] V. Fuertes, J. F. Fernández, E. Enríquez, *Optica* **6**, 668(2019).
- [9] R. Wan, S. Zhang, Z. Liu, X. Yi, L. Wang, J. Wang, J. Li, W. Zhu, J. Li, *Opt. Lett.* **44**, 4155 (2019).
- [10] Q. Chang, X. Zhou, X. Zhou, L. Chen, G. Xiang, S. Jiang, L. Li, Y. Li, X. Tang, *Opt. Lett.* **45**, 3637 (2020).
- [11] V. M. Igba, I. Ahemen, A. N. Amah, F. B. Dejene, R. Sha'Ato, A. Reyes-Rojas, J. A. Duarte-Moller, J. R. Parra-Michel, *Opt. Mater. Express* **10**, 2877 (2020).
- [12] L. Li, Y. Zhou, F. Qin, Y. Zheng, Z. Zhang, *Opt. Express* **28**, 3995 (2020).
- [13] S. Matsumoto, A. Ito, *Opt. Mater. Express* **10**, 899 (2020).
- [14] Y. Nishisu, *Int. J. Sustain. Eng.* **13**, 243 (2020).
- [15] A. Anand, R. Singh, *Sep. Purif. Rev.* **50**, 96 (2021).
- [16] H. Xie, C. Chen, J. Li, Y. He, N. Wang, *Inorg. Nano-Met.* **51**, 1297 (2021).
- [17] M. Parganiha, V. Dubey, R. Shrivastava, J. K. Synthesis, *Anal. Chem. Lett.* **11**, 719 (2021).
- [18] Z. Liu, S. Liu, K. Wang, X. Luo, *Appl. Opt.* **49**, 247 (2010).
- [19] Z. Liu, S. Liu, Kai Wang, X. Luo, *Front. Optoelec. Chin.* **2**, 119 (2009).
- [20] D. Pasinski, E. Zych, J. Sokolnicki, *J. Alloys Compd.* **668**, 194 (2016).
- [21] V. Tucureanu, A. Matei, A. M. Avram, *Opto-Electron. Rev.* **23**, 239 (2015).
- [22] Y. Kumar, Mou Pal, M. Herrera, X. Mathew, *Opt. Mater.* **60**, 159 (2016).
- [23] S. Raha, Md. Ahmaruzzaman, *Nanoscale Adv.* **4**, 1868(2022).
- [24] N. Amara, A. Martin, A. Potdevin, D. Riassetto, M. Messaoud, F. Réveret, G. Chadeyron, J. Bouaziz, M. Langlet, *J. Alloys Compd.* **842**, 155708 (2020).
- [25] J. P. C. Nascimento, F. F. do Carmo, M. X. Façanha, S. J. T. Vasconcelos, J. C. Sales, A. S. B. Sombra, *Ferroelectrics* **545**, 55 (2019).
- [26] B. Deng, J. Chen, C. Zhou, H. Liu, *Integr. Ferroelectr.* **197**, 77 (2019).
- [27] M. Rajendran, K. Singh, S. Vaidyanathan, *J. Inf. Disp.* **22**, 63 (2021).
- [28] Z. Liu, Y. Liu, C. Pan, Y. Fang, J. Hou, *Ferroelectrics* **565**, 66 (2020).
- [29] N. K. Cuong, N. Q. Khanh, *JS: MaP* **32**, 52 (2016).
- [30] S. K. Mishra, R. K. Srivastava, S. G. Prakash, R. S. Yadav, A. C. Panday, *Opto-Electron Rev.* **18**, 467(2010).
- [31] B. Sundarakannan, M. Kottaisamy, *Mater. Lett.* **165**, 153(2016).
- [32] H. H. Kim, S. Park, H. Lee, J. K. Kang, W. Choi, *Adv. Photonics Res.* **3**, 2100315 (2022).
- [33] B. Sundarakannan, M. Kottaisamy, *Ceram. Int.* **44**, 14518 (2018).
- [34] X. Yin, L. Liu, J. Yang, Z. Peng, Y. Yang, *Inorg. Nano-Met.* **49**, 198 (2019).
- [35] D. C. Awade, S. K. Omanwar, *J. Asian Ceram. Soc.* **7**, 350 (2019).
- [36] O. S. Rajamohan, V. Ponnusamy, *Mater. Res. Innov.* **23**, 402 (2019).
- [37] A. Anand, R. Singh, M. K. Ghosh, K. Sanjay, *Miner. Process. Extr. Metall.* **130**, 1 (2021).

*Corresponding author: nguyendoanquocanh@tdtu.edu.vn